DOI: 10.1002/ejic.200500690

The Coordination Chemistry of 1,4-Diazepan-6-amine[‡]

Jens Romba,[a] Dirk Kuppert,[a] Bernd Morgenstern,[a] Christian Neis,[a] Stefan Steinhauser,[a] Thomas Weyhermüller,[b] and Kaspar Hegetschweiler*[a]

Keywords: Chelates / Cobalt / Ligand design / N ligands / Stability constants

The new, tridentate, facially coordinating ligand 1,4-diazepan-6-amine (daza) has been prepared from ethane-1,2-diamine and 2,3-dibromo-1-propanol in a seven-step procedure with an overall yield of 22 %. The conformation of the free ligand has been elucidated by pH- and temperature-dependent ^{1}H NMR spectroscopy and by a single-crystal X-ray structure analysis of $H_3dazaCl_3{\cdot}H_2O$. A twisted chair with a predominantly equatorial orientation of the primary amino group has been established for daza and its protonation products H_xdaza^{x+} ($1 \leq x \leq 3$). The formation constants of $[M(daza)]^{2+}$ and $[M(daza)_2]^{2+}$ have been determined in aqueous solutions for M = Ni^{II}, Cu^{II}, Zn^{II}, Cd^{II}, and Co^{II} by potentiometric and spectrophotometric measurements, and a remarkably high stability has been found for the bis complexes ML_2 in comparison to the mono complexes ML. This effect is discussed in terms of the particular steric requirements of the daza ligand. $[Cu(daza)Cl_2]$, $[Ni(daza)_2]Cl_2{\cdot}3.2H_2O$ and $[Zn(daza)_2]SO_4{\cdot}5H_2O$ have been characterized by single-crystal X-ray analyses. Aerial oxidation of Co^{2+} in the presence of daza results in the formation of the inert $[Co(daza)_2]^{3+}$, which was isolated as a mixture of the *cis* and *trans* isomers. These two isomers were separated by chromatographic methods and identified by NMR spectroscopy and single-crystal X-ray structure analysis of *cis*-$[Co(daza)_2][ZnBr_4]Br{\cdot}H_2O$ and *trans*-$[Co(daza)_2]_3[ZnBr_4]_2Br_5{\cdot}4H_2O$. The redox potentials of $[Ni(daza)_2]^{3+/2+}$ (1.04 V vs. NHE) and $[Co(daza)_2]^{3+/2+}$ (–0.21 V vs. NHE) were determined by cyclic voltammetry. The values are slightly more positive than for corresponding complexes with related cyclic triamines. This effect is again discussed in terms of the particular steric requirements of these ligands.

1. Introduction

Triamines with a cyclic backbone and a restriction to facial coordination such as all-*cis*-1,3,5-cyclohexanetriamine (*cis*-tach),[1] 1,3,5-triamino-1,3,5-trideoxy-*cis*-inositol (taci),[2–4] or 1,4,7-triazacyclononane (tacn)[5,6] have received considerable attention in coordination chemistry. In particular, these ligands have been used to model the active site of metalloenzymes and to stabilize catalytically active metal centers.[7,8] In contrast to their open-chain aliphatic analogs, the restricted and well-defined coordination modes of the cyclic representatives allow a straightforward design of a specific coordination sphere, and the amino groups can readily be substituted with moieties carrying additional donor groups to give tetra-, penta-, or hexadentate chelators.[9–11]

The two triamines *cis*-tach and tacn may be regarded as the corner points of an entire series of triamine ligands containing a specific number of endocyclic (secondary) and exocyclic (primary) amino groups (Scheme 1). In view of the rich and interesting coordination chemistry opened up by *cis*-tach and tacn, it is rather remarkable that the intermediate members of this series have not received more attention as metal binding agents in coordination chemistry.[12–16] This is particularly surprising because asymmetric substitution of such species would easily open-up convenient routes to chiral derivatives and consequently to promising building blocks for new, enantioselective catalysts.

In two previous contributions,[14,15] we described the coordination chemistry of the two triamines *cis*-3,4-diaminopyrrolidine (*cis*-dap) and *cis*-3,5-diaminopiperidine (*cis*-dapi) and suggested that the seven-membered ring derivative 1,4-diazepan-6-amine (daza) would be a further, interesting member of this series. The use of *cis*-dapi as a building block for the construction of coordination polymers has meanwhile been described.[13] Substituted derivatives of 1,4-diazepan-6-amine are known as serotonine and dopamine receptor antagonists.[17] Moreover, a preliminary communication, proposing a 6-methyl-*N*,*N*′,*N*″,*N*‴-tetraacetic acid derivative of this compound as a potential Gd chelator for MRI applications, appeared very recently.[16] However, the unsubstituted 1,4-diazepan-6-amine ligand appears to be unknown, and to the best of our knowledge its coordination chemistry has hitherto not been investigated. We report here an efficient synthetic pathway for this interesting triamine and discuss its coordination properties with a range

[‡] Facially Coordinating Cyclic Triamines, 3. Part 2: Ref.[15]

[a] Anorganische Chemie, Universität des Saarlandes, Postfach 151150, 66041 Saarbrücken, Germany, Fax: +49-681-302-2663
E-mail: hegetschweiler@mx.uni-saarland.de
[b] Max-Planck-Institut für Bioanorganische Chemie, Postfach 101365, 45413 Mühlheim an der Ruhr, Germany

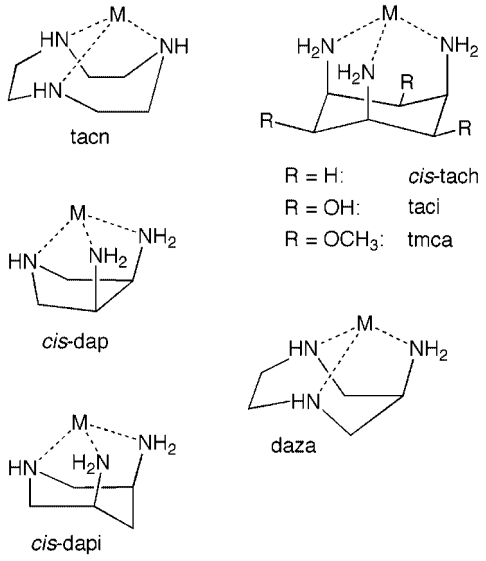

Scheme 1. Triamine ligands with a cyclic backbone.

of divalent and trivalent metal cations. The coordinating properties of the new ligand will be compared with the other cyclic triamines shown in Scheme 1, and characteristic differences will be analyzed in terms of the specific steric requirements of these compounds.

2. Results and Discussion

2.1. Preparation and Characterization of the Ligand

In previous protocols, construction of the 1,4-diazepane ring was achieved by a nitro-Mannich-type reaction.[16] We used a different approach (Scheme 2), however, and obtained the seven-membered ring by the reaction of an activated diaminoethane derivative with 2,3-dibromo-1-propanol.[18] The resulting 1,4-ditosyl-1,4-diazepan-6-ol was then transformed into the corresponding azide by converting the alcoholic OH group into a suitable leaving group followed by substitution with N_3^-.[19] Solutions of the azide were directly transferred into an autoclave and were hydrogenated to give the amine. Due to its potentially explosive nature, the isolation of the pure azide was usually avoided and only a small quantity of this compound was separated for characterization. The two remaining tosyl groups were finally removed in concd. aqueous hydrobromic acid, and the pure triamine was obtained as the trihydrochloride from a cation-exchange resin.

As expected, H_3daza^{3+} reacts as a triprotic acid. The corresponding pK_a values were determined at 25 °C by pH-metric titrations in aqueous solution for an ionic strength of 0.1 and 1 M (Table 1). The values for 0.1 M KCl and 0.1 M KNO_3 are closely related and an individual, direct interaction between the polyammonium cation and Cl^- or NO_3^- appears therefore not to be significant. The cyclic H_3daza^{3+} is more acidic than the triply protonated, open-chain 3-azapentane-1,5-diamine (H_3den^{3+}), as shown in Table 2.[20] In particular, the second pK_a value of the cyclic triamine is

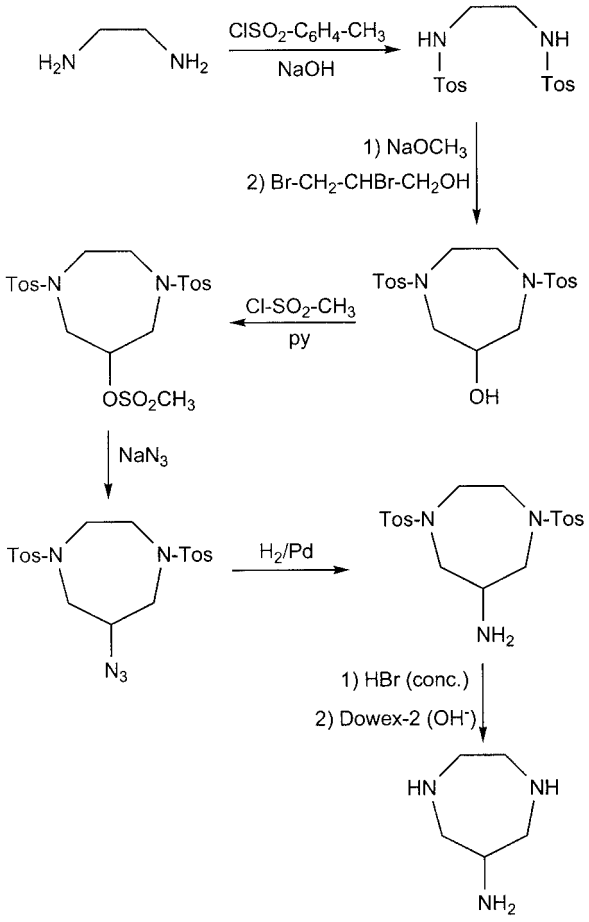

Scheme 2. Synthetic pathway for 1,4-diazepan-6-amine (daza).

considerably lower than that of the aliphatic triamine. This result is clearly a consequence of the steric constraints within the cyclic structure and can be understood in terms of simple electrostatic interactions between the positive charges located at the protonated amino groups.[15] It is also noteworthy that H_3daza^{3+} is a stronger acid than $H_3(cis\text{-}dapi)^{3+}$ (Scheme 1), with a particularly pronounced effect for the first and the second deprotonation steps. The exocyclic amino groups of such ring systems preferentially adopt an equatorial orientation,[14,21] and in terms of electrostatic repulsion, it is therefore more difficult to protonate the endocyclic amino groups. These considerations are consistent with the observation that the triply protonated 1,4,7-triazacyclononane (H_3tacn^{3+}), where exocyclic amino groups are not present, is a strong acid that is not stable in H_2O.[22]

Table 1. pK_a (= –log K_a)[a] values of H_3daza^{3+} at 25 °C.

	0.1 M KCl	0.1 M KNO_3	1.0 M KNO_3
p$K_{a,1}$	3.20	3.18	3.73
p$K_{a,2}$	6.47	6.44	6.78
p$K_{a,3}$	9.24	9.24	9.42

[a] $K_{a,i} = [LH_{3-i}] \times [H] \times [LH_{4-i}]^{-1}$. The estimated standard deviations are less than 0.01.

Structural changes of polyamines in the course of protonation can be conveniently followed by ^1H NMR spec-

Table 2. Comparison of pK_a values (25 °C, μ = 0.1 M) of representative triamines.

	H_3den^{3+} [a]	H_3tacn^{3+} [a]	H_3(*cis*-dapi)$^{3+}$ [b]	H_3(*cis*-dap)$^{3+}$ [c]	H_3daza^{3+} [d]
p$K_{a,1}$	4.3	< 2	4.2	2.4	3.2
p$K_{a,2}$	9.0	6.8	7.6	6.3	6.5
p$K_{a,3}$	9.9	10.4	9.5	9.7	9.2

[a] From ref.[20] [b] From ref.[14] [c] From ref.[15] [d] This work, Table 1.

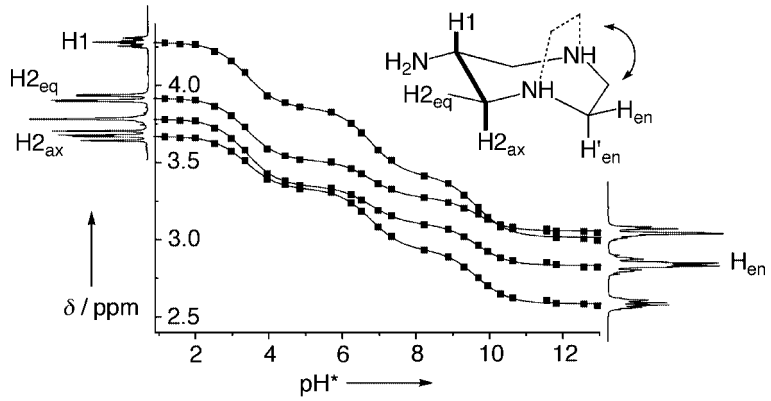

Figure 1. pH*-dependence[24] of the ^{1}H NMR resonances of H_xdaza^{x+} ($0 \le x \le 3$); squares correspond to experimental values; the lines were calculated (minimization of $[\delta_{obsd.} - \delta_{calcd.}]^2$). Inset: boat and chair conformations with averaged C_s symmetry of H_xdaza^{x+}, compatible with the NMR spectroscopic data (see text); the H1–C–C–$H2_{ax}$ fragment responsible for the large vicinal coupling constant is highlighted in bold.

troscopy.[23] A series of spectra of daza as a function of pH* was recorded at 28 °C (Figure 1).[24] Assignments were established by ^{1}H-^{1}H and ^{1}H-^{13}C 2D correlation experiments, and the δ vs. pH* curves were evaluated using a least-squares procedure. The resulting apparent pK_a values are 3.4, 6.8, and 9.7. Considering the different media (D_2O, no inert electrolyte vs. H_2O, 0.1 or 1 M KCl) these values agree well with the pK_a's obtained from the potentiometric measurements (Table 1). It is well known that C–H protons near a basic site are deshielded in the course of protonation and this effect increases with a decreasing number of bonds between the basic site and the hydrogen atom under consideration.[25] It is possible to model this effect with a suitable set of deshielding constants and this information can then be used to identify the different tautomeric forms that are possible for the partially protonated species.[14,15] Based on such considerations, we showed that the first protonation step of daza is rather unspecific, with the proton of $Hdaza^+$ almost equally distributed over the three amino groups. For H_2daza^{2+}, however, the tautomer with a protonated primary amino group is strongly predominant ($\ge$ 90%).

The determination of coupling constants as a function of pH* proved helpful to follow conformational changes in the course of deprotonation.[26] At pH* < 3, H1 appears as a well-resolved, sharp triplet of triplets with two vicinal coupling constants (J_a = 10.5 and J_b = 3.1 Hz), indicative of an axial orientation of the hydrogen atom and thus an equatorial orientation of the primary amino group. Such a conformation of H_3daza^{3+} was also observed in the crystal structure of daza·3HCl·H_2O (Figure 2), where the diazepane ring adopts a twisted chair conformation (puckering parameters: q_2 = 0.522 Å, q_3 = 0.670 Å, θ_2 = 41.4°, and θ_3 = 193.5°).[27] The coupling constants also allowed an unambiguous identification of $H2_{eq}$ and $H2_{ax}$. As expected, the hydrogen atom with an equatorial orientation appears at higher frequency. The coupling constants change slightly with increasing pH* (pH* 4: J_a = 8.4, J_b = 3.7 Hz; pH* 6: J_a = 7.4, J_b = 4.1 Hz). As is well known, the cycloheptane ring is flexible and a variety of twisted chair and twisted boat conformations of similar energy could account for the solution structure. However, the coupling constants clearly indicate that the equatorial orientation of the primary amino group is maintained in the course of deprotonation. This assumption is also supported by the observation that an intercrossing of $H2_{eq}$ and $H2_{ax}$ in the pH* range investigated has not been noted.[14,21] Moreover, recording the spectra in MeOH/H_2O (5:1) at low temperature showed only slight line broadening at 243 K, and individual signals for different conformers could not be observed.

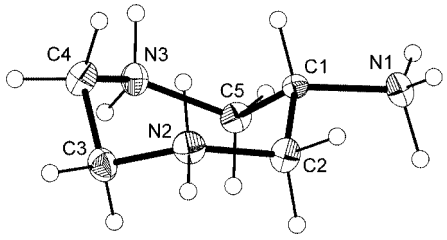

Figure 2. Molecular structure of H_3daza^{3+} showing the twisted chair conformation of the seven-membered diazepane ring. The thermal ellipsoids are drawn at the 50% probability level; hydrogen atoms are shown as spheres of arbitrary size. All bond angles and bond lengths fall in the expected ranges.

2.2. Preparation and Structural Characterization of Metal Complexes

Bis complexes of Co^{III} were prepared conventionally by aerial oxidation of the Co^{II} precursors in aqueous solution. As is well established for Co^{III}–hexaamine complexes, the resulting species proved highly inert towards ligand substitution, and they could thus be used as illustrative models for studying the properties of individual isomers. Separation of different components of the reaction mixture by means of chromatographic methods yielded two major orange products, an achiral, C_{2h}-symmetric *trans*-$[Co(daza)_2]^{3+}$ ($\mathbf{1}^{3+}$, 25%) and a chiral, C_2-symmetric *cis*-$[Co(daza)_2]^{3+}$ ($\mathbf{2}^{3+}$, 20%). The two isomers could unambiguously be identified by their NMR spectra, and this assignment was further confirmed by single-crystal X-ray structure analysis (Figure 3). The crystal structures of both complexes suffered from some disorder. In the structure of the *trans* isomer, three crystallographically independent complex molecules ($\mathbf{1a}^{3+}$, $\mathbf{1b}^{3+}$, $\mathbf{1c}^{3+}$) were located, with their metal centers Co1, Co2, and Co3 all placed on twofold rotational axes. As mentioned above, the complex cation itself is centrosymmetric. It is thus noteworthy that the three complex cations are *not* placed on a crystallographic center of inversion, even though the compound crystallizes in a centrosymmetric space group. In the complex of Co1, the ligand adopts a major and a minor orientation having occupancies of 80% and 20%, respectively. In the structure of the *cis* complex $\mathbf{2}^{3+}$, the three atoms N17, C2, and C13 are placed on a crystallographic mirror plane. All other atoms are doubled, and the entire molecule was thus found to be distributed equally over two symmetry-related positions with the above-mentioned three atoms in common.

$[Ni(daza)_2]^{2+}$ ($\mathbf{3}^{2+}$) and $[Zn(daza)_2]^{2+}$ ($\mathbf{4}^{2+}$) form immediately by the simple combination of aqueous solutions of the ligand and the hydrated metal salt. Both complexes are labile. The equilibrium between individual isomers is thus rapid and it was not possible to isolate the different isomeric species in the form of solid compounds. The two complexes $\mathbf{3}^{2+}$ and $\mathbf{4}^{2+}$ were crystallized as their chloride and sulfate salts, respectively. A single crystal structure analysis showed the *trans* form for both complexes, and two crystallographically independent complex cations ($\mathbf{4a}^{2+}$ and $\mathbf{4b}^{2+}$) were located in the structure of the Zn complex. All three complex cations $\mathbf{3}^{2+}$, $\mathbf{4a}^{2+}$, and $\mathbf{4b}^{2+}$ lie on crystallographic centers of inversion, and we attribute the exclusive observation of the *trans* form to better packing of the centrosymmetric isomer.

A comparison of bond lengths and bond angles within the coordination spheres of the bis complexes $\mathbf{1a}^{3+}$–$\mathbf{1c}^{3+}$, $\mathbf{2}^{3+}$, $\mathbf{3}^{2+}$, $\mathbf{4a}^{2+}$, and $\mathbf{4b}^{2+}$ indicates some characteristic deviation from an ideal octahedral geometry. Intraligand N–M–N angles are generally smaller than 90° and interligand N–M–N angles are larger than 90°. This effect increases with the increasing ionic radius of the metal center. Moreover, the M–N bonds of the primary (exocyclic) amino groups are somewhat shorter than the M–N bonds of the secondary (endocyclic) amino groups (Table 3). We regard this effect as a consequence of the steric constraints of the ligand framework rather than a result of the different donor capacity of the two types of nitrogen donors (the secondary nitrogen donor is usually considered to be a stronger nucleophile).

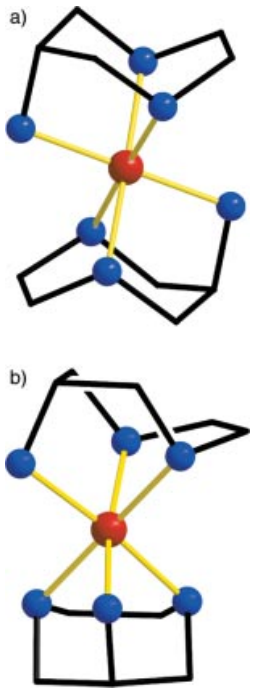

Figure 3. Molecular structure of a) the *trans*- and b) the *cis*-isomer of $[Co(daza)_2]^{3+}$ ($\mathbf{1}^{3+}$ and $\mathbf{2}^{3+}$). Color code: Co brown, N blue; the carbon skeleton is shown as a stick model (black); hydrogen atoms have been omitted for clarity. $[Ni(daza)_2]^{2+}$ ($\mathbf{3}^{2+}$) and $[Zn(daza)_2]^{2+}$ ($\mathbf{4}^{2+}$) adopt virtually the same *trans* structure as shown for the Co^{III} complex $\mathbf{1}^{3+}$ (a).

The reaction of hydrated $CuCl_2$ with an excess of daza in aqueous solution resulted in the formation of a mononuclear, neutral 1:1 complex $[Cu(daza)Cl_2]$ (**5**). A crystal-structure analysis of this compound revealed a coordination number of five with a distorted square-pyramidal geometry (τ = 0.04).[28] Again, the intraligand N–Cu–N angles are significantly smaller than 90° and this effect mainly contributes to the deviation of the complex geometry from an ideal square pyramid. Complex **5** and the previously reported $[Cu(cis\text{-dapi})Cl_2]$ have closely related structures. In both complexes, the two chloro ligands and two of the nitrogen donors form the basal plane of the square pyramid. The third nitrogen donor is placed at the apex and has a considerably longer Cu–N bond (Table 3). In both structures, it is the endocyclic (secondary) nitrogen donor which forms this long bond to the apical position (Figure 4). With regard to the number of endocyclic and exocyclic nitrogen donors, the two triamine ligands *cis*-dapi (two exocyclic one endocyclic nitrogen atoms) and daza (one exocyclic, two endocyclic nitrogen atoms) are complements, and this is clearly reflected in the molecular structures of $[Cu(daza)Cl_2]$ and $[Cu(cis\text{-dapi})Cl_2]$. The free ligands *cis*-dapi and daza are both bisected by a mirror plane (C_s symmetry);

Table 3. Synopsis of structural parameters of H_3daza^{3+}, *cis*-$[Co(daza)_2]^{3+}$, *trans*-$[Co(daza)_2]^{3+}$, $[Ni(daza)_2]^{2+}$, $[Cu(daza)Cl_2]$, and $[Zn(daza)_2]^{2+}$.

	$M–N_{exo}$ (min., max., mean) [Å]	$M–N_{endo}$ (min., max., mean) [Å]	$N_{endo}–C–C–N_{endo}$ torsional angles [°]	Puckering parameters[27] q_2 [Å]	q_3 [Å]	θ_2 [°]	θ_3 [°]	Q [Å]
H_3daza^{3+}			88.4	0.52	0.67	41	194	0.85
cis-Co-daza	1.946(8)	1.977(8)	0.5	0.59	0.72	337	50	0.93
	1.971(7)	2.002(6)	4.9	0.60	0.71	341	52	0.93
	1.959	1.985						
trans-Co-daza[a]	1.947(3)	1.956(3)	6.3 (Co2)	0.61	0.70	341	53	0.93
	1.952(3)	2.004(3)	0.3 (Co3)	0.60	0.70	336	51	0.92
	1.950	1.980						
Ni-daza		2.136(3)	0.1	0.57	0.68	334	52	0.88
		2.137(2)						
	2.108(3)	2.137						
Cu-daza		2.117(9)	9.8	0.56	0.69	345	54	0.89
		2.376(9)						
	1.970(11)	2.247						
Zn-daza	2.147(3)	2.194(2)	2.2 (Zn1)	0.56	0.67	332	51	0.87
	2.148(3)	2.234(2)	1.4 (Zn2)	0.55	0.66	336	52	0.86
	2.148	2.215						

[a] Only the nondisordered ligands are considered.

however, this mirror plane is only retained in the *cis*-dapi complex, while the daza complex is devoid of any symmetry (C_1).

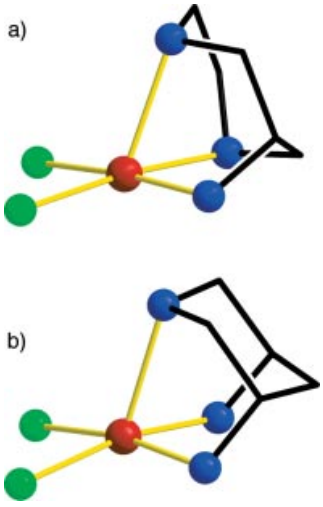

Figure 4. Molecular structure of a) $[Cu^{II}(daza)Cl_2]$ (**5**) and b) $[Cu^{II}(cis\text{-dapi})Cl_2]$ (from ref.[14]). Color code: Cu brown, N blue, Cl green; the carbon skeleton is shown by a stick model (black); hydrogen atoms have been omitted for clarity.

In all the complexes reported here the seven-membered diazepane ring adopts a regular chair conformation as indicated by the four puckering parameters q_2, q_3, θ_2, and θ_3 (Table 3).[27] This structural type is imposed by the tridentate coordination mode and implies an almost eclipsed orientation of the $N–CH_2–CH_2–N$ fragment (Table 3). It is noteworthy that the conformation of the corresponding five-membered chelate rings differs markedly from the well known λ/δ conformation observed in complexes with the open-chained ethane-1,2-diamine (Scheme 3), and also from the conformation that has been found for the noncoordinated ligand (Figure 2). It is thus obvious that a tridentate coordination mode of daza enforces some torsional strain within the metal complex.

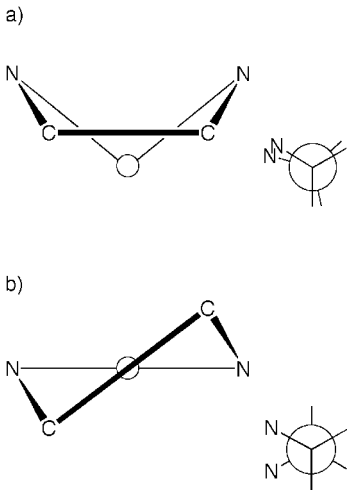

Scheme 3. Conformation of five-membered chelate rings in a metal complex with daza (a) and the open-chained ethane-1,2-diamine (b).

2.3. Stability of the Metal Complexes

The formation constants of daza complexes with Co^{II}, Ni^{II}, Cu^{II}, Zn^{II}, and Cd^{II} were measured in aqueous media by potentiometric methods (Figure 5). A summary of these results is presented in Table 4. The main species formed in solution are $[M(daza)]^{2+}$ and $[M(daza)_2]^{2+}$. For Cu^{II}, however, formation of the protonated $[Cu(Hdaza)]^{3+}$ and $[Cu(daza)(Hdaza)]^{3+}$ was also verified unambiguously. As shown by their pK_a values of 3.82 and 4.67, the two protonated complexes behave as acids of moderate strength.

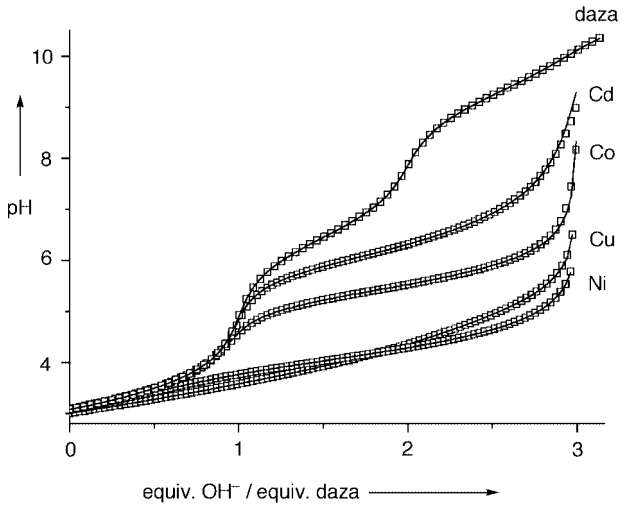

Figure 5. Titration curves (25 °C, 0.1 M KCl) of daza in the presence and absence of divalent metal cations as indicated. The total daza concentration is 2×10^{-3} M, and (if present) the total metal concentration is 10^{-3} M. Squares refer to experimental values, the lines were calculated using the formation constants listed in Tables 1 and 4. The curve of the Zn complex is similar to the Co complex and has been omitted for clarity.

Table 4. Formation constants ($\log \beta_{xyz}$)[a] of daza (= L) complexes (25 °C, μ = 0.1 M).

	$M(L)^{2+}$ $\log \beta_{110}$	$M(HL)^{3+}$ $\log \beta_{111}$	$M(L)_2^{2+}$ $\log \beta_{120}$	$M(L)(HL)^{3+}$ $\log \beta_{121}$
Co	7.85(1)	–	15.29(1)	–
Zn	7.44(1)	–	14.21(1)	–
Cu	11.07(2)	14.89(2)	20.45(1)	25.12(4)
Ni	10.53(1)	–	20.53(1)	–
Cd[b]	6.49(2)	–	11.65(2)	–
Cd[c]	6.47(2)	–	12.22(2)	–

[a] $\beta_{xyz} = [M_xL_yH_z] \times [M]^{-x} \times [L]^{-y} \times [H]^{-z}$. The uncertainties given in parentheses correspond to 3σ. [b] 0.1 M KCl; the expression [M] and [ML] in the previous footnote should be interpreted as $\Sigma[MCl_i]$ and $\Sigma[MLCl_i]$, i = 0, 1, respectively, see Section 2.3. [c] 0.1 M KNO_3.

It is well known that complexes with rigid ligands, having a cyclic backbone, often undergo ligand-exchange reactions that are slow relative to related ligands that do not have the same steric constraints. Moreover, comparatively slow substitution characteristics are well established for the Ni^{II} center. Consequently, Ni^{II}–amine complexes such as $[Ni(cis\text{-tach})]^{2+}$ are inert,[29] and equilibration during a titration experiment is slow. In our previous investigations, a series of batch titrations were performed to investigate the Ni^{II}-*cis*-dapi, Ni^{II}-tmca, and Ni^{II}-taci system in aqueous solution.[14,21,30] In the Ni^{II}-daza system reported here, we therefore checked for complete equilibration by performing back titrations. To our surprise, the Ni^{II}-daza complexes proved to be labile, and an equilibration time of a few minutes after addition of an increment of titrant was sufficient even in the acidic range of the titration curve! It is well known that seven-membered rings readily undergo conformational changes, whereas six-membered chair structures, such as those observed in *cis*-dapi or taci, are rigid. The different flexibility of these ligand backbones obviously accounts for the variable lability of these tridentate systems.

In some of the titration experiments of the Ni^{II} and Cu^{II} complexes, the titration cell was equipped with an immersion probe, which was connected to a spectrophotometer with a diode array detector. This allowed the acquisition of additional spectrophotometric data, which were used to confirm the applied model and to evaluate the formation constants by an independent method (Figure 6). Moreover, the spectra of the individual species, which were calculated from the data, provided valuable information about the nature of the coordinated donor set. Due to the low intensity of the observed d–d transitions, the total metal concentration was increased to 10 mM and the inert electrolyte concentration was set at 1.0 M.

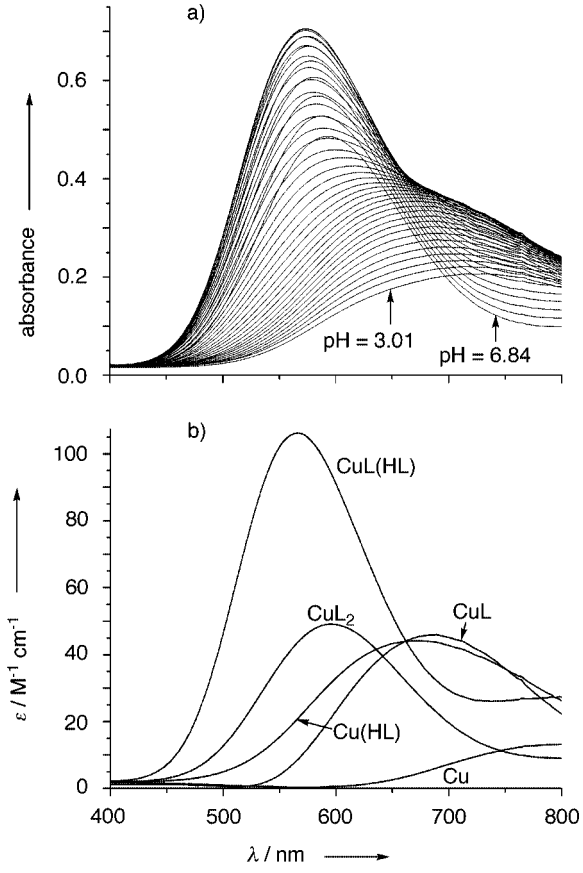

Figure 6. Determination of the formation constant $\log \beta_{xyz}$ of $[Cu_x(daza)_yH_z]^{2x+z}$ by spectrophotometric methods: a) the sample spectra of the spectrophotometric titration with total Cu/total daza = 1:2 in the range $3.0 < pH < 6.8$; b) calculated spectra of the individual $[Cu_x(L)_yH_z]^{2x+z}$ species (L = daza). The spectra of Cu^{2+} was measured separately and was imported without refinement. The free ligand and its protonation products were considered as colorless.

As shown in Table 5, the agreement between the potentiometric and spectrophotometric measurements is generally good. $[Ni(daza)]^{2+}$ and $[Ni(daza)_2]^{2+}$ both exhibit the well-known three bands of a d^8 electron configuration, with maxima of the middle band [$^3A_{2g} \rightarrow {}^3T_{1g}(F)$ transition] at 590 and 513 nm, respectively. These values strongly sup-

port an octahedral triamine-triaqua-Ni^{II} and hexaamine-Ni^{II} chromophore, respectively (Figure 7),[31] and confirm that the tridentate coordination mode of daza observed in the crystal structure of $[Ni(daza)_2]Cl_2 \cdot 3.2H_2O$ is retained in solution. The Cu^{II} complexes all show a single, broad, unresolved band. For $[Cu(daza)(Hdaza)]^{3+}$, the maximum of this band is found at 566 nm. Such a value is characteristic of a CuN_4 chromophore with all four nitrogen donors occupying equatorial positions, and one or two additional, weakly bonded H_2O molecules in apical positions.[32] $[Cu(daza)_2]^{2+}$ exhibits a maximum at 596 nm. The corresponding red shift of about 30 nm, which follows from deprotonation of $[Cu(daza)(Hdaza)]^{3+}$, is very characteristic of the coordination of one additional nitrogen donor in one of the apical positions ("pentaamine effect").[23,33] Coordination of a sixth nitrogen donor obviously does not take place, because the maximal absorption for a tetragonally elongated CuN_6 chromophore would appear at even higher wavelength (around 620–640 nm).[31] As a result, we have assigned a bis-didentate coordination mode to the protonated $[Cu(daza)(Hdaza)]^{3+}$ and a combination of a didentate and tridentate coordination mode to $[Cu(daza)_2]^{2+}$. The protonated mono complex $[Cu(Hdaza)]^{3+}$ also absorbs at somewhat shorter wavelength than the nonprotonated $[Cu(daza)]^{2+}$. For these two species, the difference in wavelength is, however, relatively minor. For $Hdaza^+$, only didentate coordination is reasonable, and the red shift observed upon deprotonation is again indicative of a tridentate coordination mode for daza. Such a coordination mode is the same as that which has been observed in the solid-state structure of $[Cu(daza)Cl_2]$ (Figure 4). However, a comparison of the stability constants of $[Cu(en)]^{2+}$ ($\log \beta = 10.5$) and $[Cu(daza)]^{2+}$ ($\log \beta = 11.1$) reveals only a minor increase in stability upon going from the didentate to the tridentate ligand systems ($\Delta \log \beta = 0.6$). Obviously, the third nitrogen donor of daza undergoes only weak binding to the Cu^{II} center. This is in marked contrast to the Ni^{II} system, where $[Ni(daza)]^{2+}$ is considerably more stable than $[Ni(en)]^{2+}$ ($\Delta \log \beta = 3.2$).[15]

Table 5. Comparison of formation constants[a] of Ni^{II}– and Cu^{II}–daza complexes derived either from potentiometric (pot) or spectrophotometric (spec) titrations (25 °C, 1 M KNO_3) together with spectrophotometric data. Estimated standard deviations (3σ) are given in parentheses.

	x,y,z	$\log \beta_{xyz}$ (pot/spec)	λ_{max} [nm]/ε [$M^{-1}cm^{-1}$]
$[Cu(daza)]^{2+}$	1,1,0	11.19(3)/11.33(9)	682/45
$[Cu(Hdaza)]^{3+}$	1,1,1	15.43(1)/15.52(6)	674/44
$[Cu(daza)_2]^{2+}$	1,2,0	20.76(1)/20.91(6)	596/49
$[Cu(Hdaza)(daza)]^{3+}$	1,2,1	25.95(2)/26.06(6)	566/108
$[Ni(daza)]^{2+}$	1,1,0	10.72(1)/10.7(1)	590/8
$[Ni(daza)_2]^{2+}$	1,2,0	20.85(1)/20.9(1)	513/11

[a] $\beta_{xyz} = [M_xL_yH_z] \times [M]^{-x} \times [L]^{-y} \times [H]^{-z}$.

As noted previously for *cis*-dapi,[14] the formation constants measured for the bis complex $[Cd(daza)_2]^{2+}$ are significantly different in 0.1 M KCl or 0.1 M KNO_3, whereas the formation constants of the mono complex are virtually the same in the two media. This result can be explained in terms of the formation of the chloro complexes $[CdCl]^+$ and $[Cd(daza)Cl]^+$. The formation constant of $[CdCl]^+$ is known to be $K^{Cl} = [CdCl^+] \times [Cd^{2+}]^{-1} \times [Cl^-]^{-1} = 33\ M^{-1}$.[20] Conditional constants of the type $\beta_i^{cond} = \{[CdL_i] + [CdL_iCl]\} \times \{[Cd]+[CdCl]\}^{-1} \times [L]^{-i}$ may be used to describe the equilibria in the chloride medium, and $\beta_1^{cond} = \beta_1$ is thus indicative of approximately the same affinity of Cd^{2+} and $CdCl^+$ for the binding of one daza ligand. The difference between β_2 and β_2^{cond} corresponds to the value of $K^{Cl} \times [Cl^-]$ within experimental error, and this result demonstrates that $[Cd(daza)_2]^{2+}$ does not interact directly with Cl^- to a significant extent, which lends strong support for a coordination number of six within the hexaamine complex.

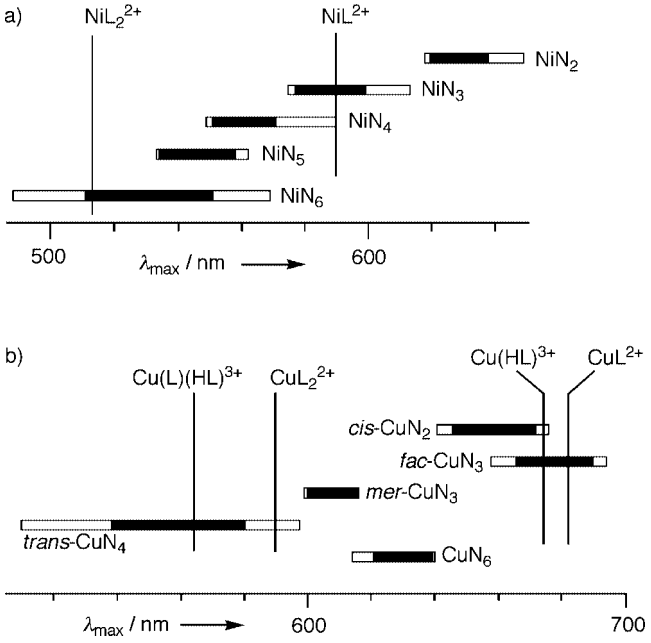

Figure 7. Correlation of the observed λ_{max} values of the individual a) Ni^{II}– and b) Cu^{II}–daza complexes formed in aqueous solution with the λ_{max} values of some chromophores reported in the literature.[31] Only complexes with a defined coordination environment containing a set of sp^3-nitrogen donors as indicated and H_2O as additional ligands were considered. The data of the Ni^{II} complexes refer to the $^3A_{2g}$–$^3T_{1g}(F)$ transition. Open boxes refer to the entire range reported, black boxes represent the averages ± one standard deviation.

A synopsis of the formation constants for some representative cyclic triamine ligands is given in Figure 8. The following general trends are noteworthy:

(i) With the exception of tacn, all the ligands shown have a remarkably low affinity for Cu^{II} in comparison to Ni^{II}. For *cis*-tach, daza, and *cis*-dapi, $[Cu^{II}L]^{2+}$ is only of slightly higher stability than $[Ni^{II}L]^{2+}$ (Figure 8a). For 1,3,5-triamino-1,3,5-trideoxy-*cis*-inositol (taci), and its *O*-methylated derivative *all-cis*-2,4,6-trimethoxycyclohexane-1,3,5-triamine (tmca), the Irving–Williams order is even inverted, and the Ni complex is more stable. This effect is markedly

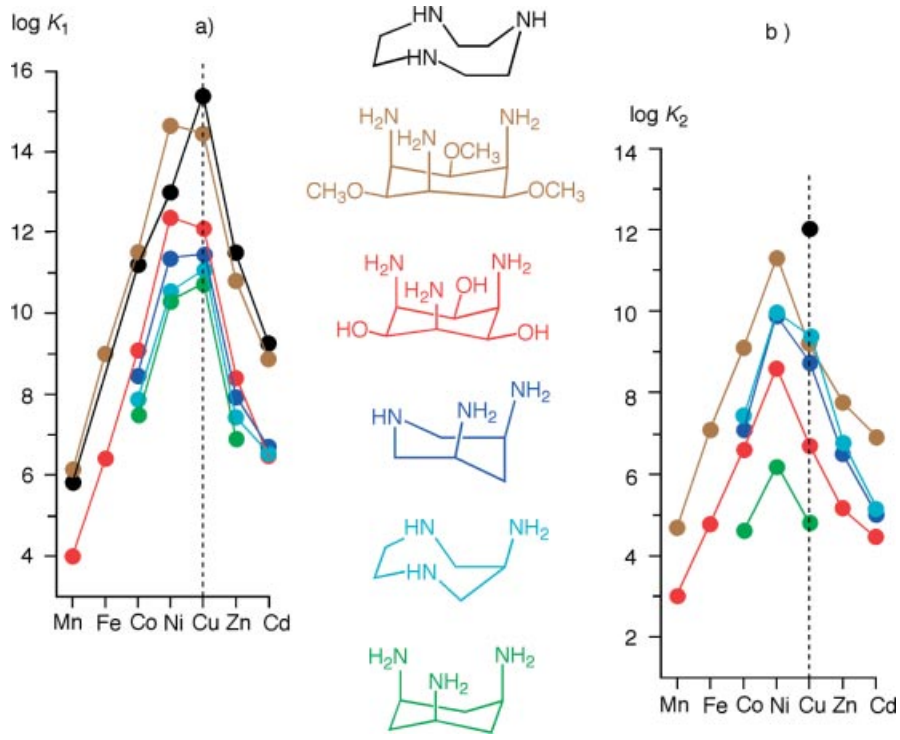

Figure 8. Survey of formation constants for complexes with divalent cations and various cyclic triamine ligands as indicated. Note that the values of the individual formation constants ($K_1 = [ML] \times [M]^{-1} \times [L]^{-1}$ and $K_2 = [ML_2] \times [ML]^{-1} \times [L]^{-1}$) rather than overall constants (β_1 and β_2) are shown. The constants of the daza complexes are from this work (Table 4), the formation constants of the other ligands are from refs.[3,14,20,21,36]

more pronounced for the addition of a second ligand moiety (Figure 8b), where a distinct maximum is now observed at Ni^{II} for all the ligands. The preferred binding of Ni^{II} is obviously due to the exclusive facial coordination mode of these ligands, which results in the above-mentioned weak binding of the third amine donor to the Cu^{II} center.

(ii) In comparison to the other cyclic triamine ligands, the stability of the $[M(daza)]^{2+}$ species is generally low. As a matter of fact, only *cis*-tach forms 1:1 complexes of slightly lower stability. The relatively poor stability of the *cis*-tach complexes, and to a lesser extent of the *cis*-dapi complexes, is readily understood in terms of the high-energy conformation (primary amino groups all in axial positions), which is required for complex formation.[34] For taci and tmca, both chair conformations are destabilized by 1,3-diaxial repulsive interactions and metal binding does thus not require such an additional amount of energy. For daza, the primary amino group in the free ligand also has a preferred equatorial orientation (see Section 2.1), however, compared to *cis*-tach and *cis*-dapi, one would expect that much less energy is needed to bring it into an axial position. As already outlined in Section 2.2, it is the enforcement of the unfavorable chair conformation of the diazepane ring (local C_s symmetry) with the eclipsed arrangement of the N_{endo}–CH_2–CH_2–N_{endo} fragment that accounts for the low stability.

(iii) In contrast to the relatively low stability of the $[M(daza)]^{2+}$ complexes, the binding of a second ligand moiety (formation of $[ML_2]^{2+}$) is a highly favored process (Figure 8b). The ratio $\log K_1/K_2$ for the cyclohexane-based ligands *cis*-tach, taci, and tmca (excluding Cu^{II}) lies in the range of 2.0–4.1, whereas for daza it is 0.4–0.7. A similar behavior has previously been reported for *cis*-dapi ($\log K_1/K_2 \approx 1.4$),[14] although the ratio observed for daza is even smaller. A purely statistical approach would require that $K_1/K_2 = 16$ ($\log K_1/K_2 = 1.2$),[35] and thus it is evident that the two ligands in the $[M(daza)_2]^{2+}$ complexes show some cooperativity. As discussed previously,[14,36] the different behavior of the ligands with three exocyclic amino groups on the one hand and of *cis*-dapi and daza on the other can be explained by means of steric requirements, which result in different interligand interactions (Scheme 4). Moreover, some symbiotic behavior appears to further enlarge the binding of the second ligand.[37] The high cooperativity between the two ligand moieties in the $[M(daza)_2]^{2+}$ complexes results in some effects that are rather unusual in solution chemistry (Figure 9). For example, for ligands such as tmca, with "normal" behavior, $[ML]^{2+}$ is usually the only species that is present to a significant extent in solutions with equal concentrations of total ligand and total metal, and formation of $[ML_2]^{2+}$ is generally negligible. Furthermore, in solutions with a total metal/total ligand concentration of 1:2, the mono complex appears as the dominant species in the acidic range. In contrast, for daza, significant amounts of $[ML_2]^{2+}$ already form up to 30% in solutions with equal concentrations of total M and total L according to $2ML \rightarrow M + ML_2$, and in solutions with excess ligand $[ML]^{2+}$ appears only as a minor species within a narrow pH range.

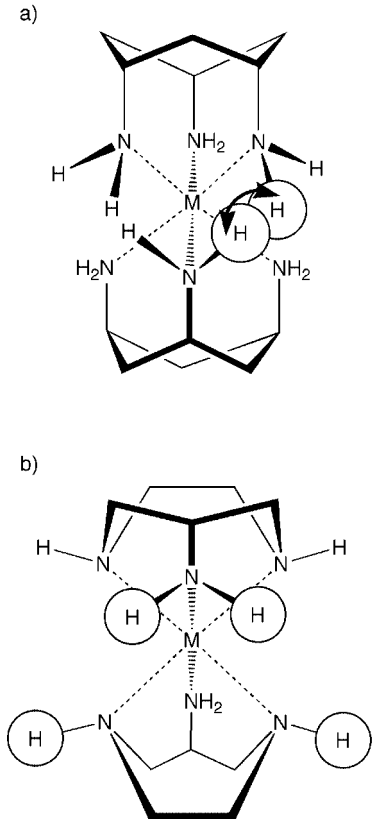

Scheme 4. Interligand repulsion in bis complexes ML_2 [L = *cis*-tach (a) and daza (b)].

2.4. Redox Properties

The redox properties of $[Co(daza)_2]^{3+/2+}$ and $[Ni(daza)_2]^{3+/2+}$ were investigated by means of cyclic voltammetry. For comparison, corresponding complexes with *cis*-dapi and taci were also studied. All the complexes investigated revealed quasi-reversible redox behavior (Figure 10), and the peak current was found to be linearly dependent on the square root of the scan rate, as expected for a diffusion-controlled process (Table 6). For the investigation of the $[Co(daza)_2]^{3+/2+}$ couple, crystalline samples of the distinct Co^{III} complexes were used for the preparation of the test solutions. The *cis*- and the *trans*-isomers were investigated

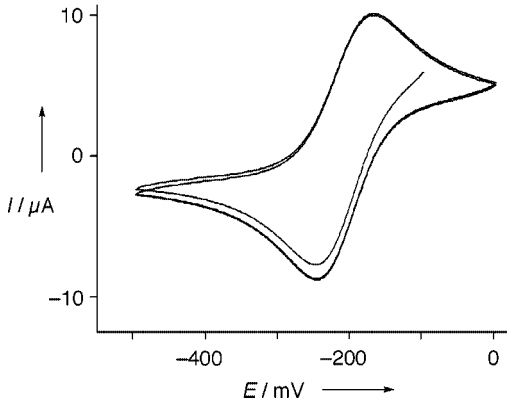

Figure 10. Cyclic voltammogram of $[Co(daza)_2]^{3+/2+}$ in aqueous solution (referenced against NHE, pH 10, 25 °C, v = 50 mV s^{-1}).

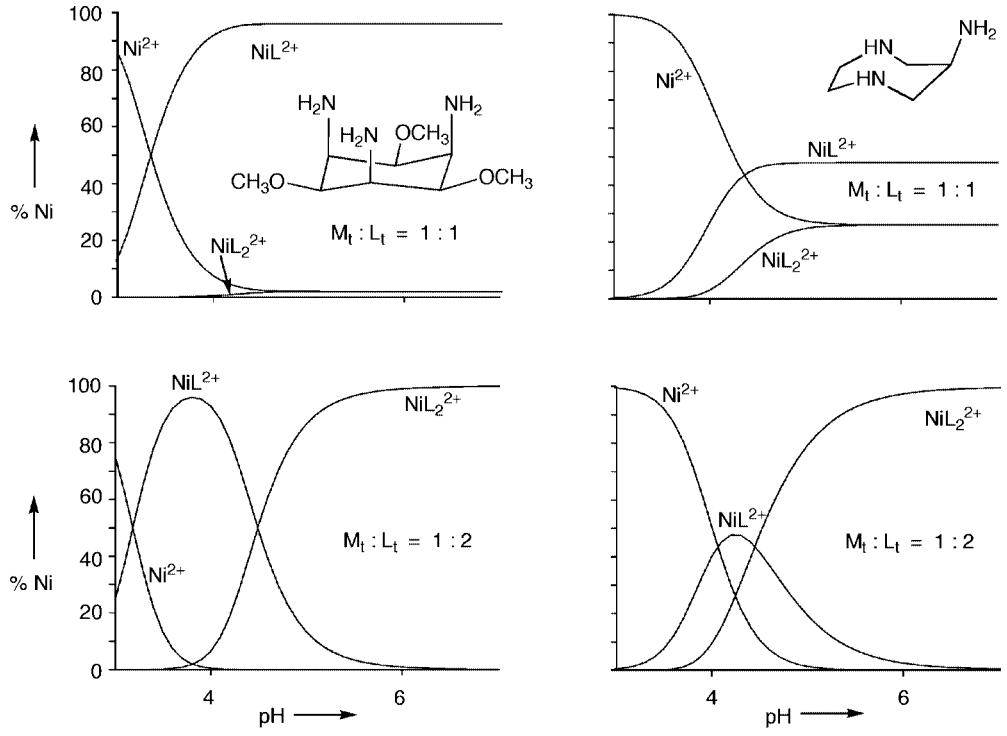

Figure 9. Illustration of the different solution properties for triamine complexes with a low (left side) and a high (right side) cooperativity between the two ligand moieties in a 1:2 complex. The species distribution was calculated for a total metal concentration of 10^{-3} M and a total ligand concentration of 10^{-3} M (top) and 2×10^{-3} M (bottom). The formation constants used for the Ni^{II}–daza system are from this work (Table 4), the formation constants of 2,4,6-trimethoxy-1,3,5-cyclohexanetriamine are from ref.[21]

separately; however, the cyclic voltammograms of the two isomers did not differ to a significant extent. A similar observation has previously been reported for the $[Co(cis\text{-dapi})_2]^{3+/2+}$ system.[14]

Table 6. Electrochemical data from cyclic voltammetry for the $[CoL_2]^{3+/2+}$ and $[NiL_2]^{3+/2+}$ couples in aqueous solution.

$[ML_2]^{3+/2+}$	$E_{1/2}$ [V][a]	ΔE_p [mV][b]	R[c]
$[Co(daza)_2]^{3+/2+}$	–0.21	74, 95	0.9998
$[Co(taci)_2]^{3+/2+}$	–0.35	75, 114	0.9995
$[Co(cis\text{-dapi})_2]^{3+/2+}$	–0.38	69, 91	0.9999
$[Ni(daza)_2]^{3+/2+}$	1.04	86, 132	0.9978
$[Ni(taci)_2]^{3+/2+}$	0.95	76, 98	0.9999
$[Ni(cis\text{-dapi})_2]^{3+/2+}$	0.92	72, 94	0.9999

[a] Reduction potentials relative to NHE. [b] Peak separation for a scan rate of 20 mV s^{-1} and 1000 mV s^{-1}, respectively. [c] Correlation coefficients for the linearity of I vs. $\sqrt{(v)}$ in the range 20 mV s^{-1} $\leq$ v $\leq$ 1000 mV s^{-1} with a total of eight data points for each couple.

In general, the reduction potentials of corresponding *cis*-dapi and taci complexes are in close agreement, whereas the redox potentials of the daza complexes are all somewhat more positive (Table 6). Obviously, the taci- and *cis*-dapi- (= L^a) complexes with divalent cations are stronger reducing agents than corresponding daza (= L^b) complexes, and this means that in a taci- or *cis*-dapi complex the trivalent cation is stabilized according to

$$\Delta E_{1/2} = E_{1/2}(L^a) - E_{1/2}(L^b) = -RT/F \times \{\ln[\beta_2^{III}(L^a)/\beta_2^{II}(L^a)] - \ln[\beta_2^{III}(L^b)/\beta_2^{II}(L^b)]\} = -RT/F \times \Delta\ln(\beta_2^{III}/\beta_2^{II})$$

where β_2^{III} and β_2^{II} stand for the formation constants of the bis complexes with the trivalent and divalent cations, respectively. For *cis*-dapi and daza, one obtains $\Delta\log(\beta_2^{III}/\beta_2^{II}) = 2.9$ for $Co^{III/II}$ and 2.0 for $Ni^{III/II}$. It is interesting to note that Hancock has proposed some characteristic size selectivity for five- and six-membered chelate rings. The steric constraints of five-membered chelate rings are more suited for the binding of a large metal cation, whereas formation of six-membered chelate rings is more favorable for small cations.[38] Since the higher oxidation state generally implies a smaller ionic size, one would thus expect a less-negative redox potential for a ligand forming exclusively five-membered chelate rings, and that is indeed what we observe. The somewhat smaller $\Delta\log(\beta_2^{III}/\beta_2^{II})$ value of Ni (in comparison to Co) can be attributed to the well-known Jahn–Teller distortion caused by the low-spin d^7 electron configuration. This type of distortion would destabilize the Ni^{III} complex with a cyclic triamine ligand in a similar way as described for Cu^{II} (see Section 2.3),[23] and this effect is obviously more pronounced for the rigid taci or dapi than for daza.

3. Conclusions

In this paper, we have shown that 1,4-diazepan-6-amine (daza) readily forms 1:1 and 1:2 complexes with divalent transition metal cations in aqueous solution and exhibits mainly a tridentate facial coordination mode. The specific coordinating properties of daza are as follows:

a) In contrast to the C_{3v}-symmetric representatives such as tacn or *cis*-tach (Scheme 1), the C_s-symmetric ligand daza (similar to *cis*-dapi) is of lower symmetry and thus gives rise to a more complex stereochemistry. In particular, bis complexes exist in the form of *cis*- and *trans*-isomers. Due to the labile nature of most of the metal centers used, the different forms equilibrate rapidly and cannot be isolated. For the inert Co^{III}, we obtained approximately equal amounts of *cis*-$[Co(daza)_2]^{3+}$ and *trans*-$[Co(daza)_2]^{3+}$ which indicates that the energy of the two isomers does not differ significantly.

b) In comparison with other triamine ligands, the stability of the complexes is not exceptionally high. As an example, the open-chained 3-azapentane-1,5-diamine (den) forms a NiL^{2+} complex with a formation constant, $\log \beta_1$, of 10.55,[20] which corresponds closely to the value (10.53) found for daza (Table 4). This result was somewhat unexpected because the donor set of the daza ligand has a much higher degree of pre-orientation. In comparison to other cyclic ligands (Scheme 1), the stability of daza complexes is relatively poor. We attribute the lower stability to the unfavorable, eclipsed conformation of the N_{endo}–CH_2–CH_2–N_{endo} moiety, which is enforced in the course of coordination. In making comments about apparent stability, however, one should note that daza is a much weaker base than, for instance, the open-chained den, and although the formation constants of the two triamines are similar, daza is a much more effective chelator in neutral or slightly acidic media.[15]

c) The cooperativity between two daza moieties of a bis complex is even higher than for *cis*-dapi, and, as a consequence, a significant amount of the bis complex is formed already if the ligand and the metal are added in a 1:1 ratio. With regard to possible applications (catalysis, modeling of the active site of a metalloenzyme), as outlined in the introduction, this high cooperativity is disadvantageous − binding of a substrate requires at least one free coordination site and the formation of the bis complexes should thus be avoided.[39] This problem can, however, be solved by adding additional substituents to some of the nitrogen donors in such a way that the steric demands, and thus interligand repulsion, disfavor the binding of a second ligand entity. This topic will be the issue of a subsequent paper.[40]

d) Compared to the *cis*-tach and *cis*-dapi backbone, the daza backbone appears to be rather flexible and this results in fast ligand-substitution behavior. The kinetics of ligand formation, although not yet studied in detail, resemble that of an open-chained ligand system.

e) The daza ligand exclusively forms five-membered chelate rings and this favors complex formation with relatively large cations. As a consequence, the redox potential of $M^{III}(daza)_x/M^{II}(daza)_x$ couples is somewhat more positive (less negative) than corresponding couples with *cis*-dapi or taci complexes.

Experimental Section

General: The commercially available chemicals used for the synthetic work were of reagent grade quality and were used as obtained. DMSO was from Fluka (puriss., p. a.). MeOH and EtOH were purified by distillation prior to use. Dowex 50 W-X2 (100–200 mesh, H^+ form) and Dowex 2-X8 (50–100 mesh, Cl^- form) were from Fluka. The anion resin was converted into the OH^- form by treatment with 0.3 M aqueous NaOH. For the potentiometric and spectrophotometric titrations, metal salts of highest available quality (>99.95%) were used. H_2O was distilled twice (quartz apparatus). UV/Vis spectra of the Co^{III} complexes were measured with an Uvikon 941 spectrophotometer (H_2O, 25 ± 3 °C). IR spectra were recorded with a Bruker Vector 22 FT IR spectrometer equipped with a Golden Gate ATR unit. Semi-quantitative determinations of Co^{II} in solution were performed with Merckoquant 10002 test strips (Merck). C,H,N analyses were performed by H. Feuerhake (Universität des Saarlandes).

NMR: ^1H and $^{13}C\{^1H\}$ NMR spectra were measured in [D_6]-DMSO, CD_3OD, or D_2O at 28 °C using a Bruker DRX Avance 400 MHz NMR spectrometer (resonance frequencies: 400.13 MHz for ^1H and 100.6 MHz for $^{13}C\{^1H\}$). Chemical shifts are given in ppm relative to [D_4]sodium (trimethylsilyl)propionate (D_2O) or tetramethylsilane ([D_6]DMSO and CD_3OD) as internal standards (δ = 0 ppm). A Hamilton SPINTRODE glass electrode, which was calibrated with aqueous (H_2O) buffer solutions, was used to measure pH* directly in the NMR tube.[24] The pH* of each sample was adjusted with appropriate solutions of DCl and NaOD in D_2O.

Cyclic Voltammetry: Cyclic voltammograms were recorded at ambient temperature (25 ± 2 °C) in a BAS C2 cell (0.5 M KCl), using a BAS 100B/W2 potentiostat, a gold (for the Co complexes) or glassy carbon (for the Ni complex) working electrode, a platinum counter electrode, and an Ag/AgCl reference electrode. Sample solutions of the Co complexes were made up using solid $[CoL_2]^{3+}$ salts. The total Co concentration was 0.004 M and the pH was adjusted to 10 (KOH). Ni samples were prepared in situ using a Ni^{II} salt and the trihydrochloride of the ligands (total Ni^{II} = 0.012 M, total L = 0.03 M, L = daza, taci, *cis*-dapi). 0.5 M KOH was then added to bring the pH to a value of 7.

Potentiometric and Spectrophotometric Measurements: The titration experiments were performed at 25.0 °C under N_2 or Ar (for the Co complexes) as described previously.[41] Simple potentiometric titrations were carried out with total M/total daza ratios of 1:1 and 1:2 in 0.1 M KCl or 0.1 M KNO_3 (Figure 5). Titration experiments, which were followed by potentiometric and spectrophotometric methods, were performed in 1 M KCl. A Metrohm 665 piston burette was used for addition of the titrant (KOH, HCl or HNO_3), and the pH was recorded using a Metrohm glass electrode with an incorporated Ag/AgCl reference, connected to a Metrohm 713 pH/mV meter. For spectrophotometric measurements, the titration cell was equipped with an immersion probe (HELLMA), which was connected to a spectrophotometer equipped with a diode array detector (J&M, TIDAS-UV/NIR/100-1). The titrations were performed with a total metal concentration of 0.01 M and a total daza concentration of 0.02 M. A PC was used to trigger recording of a spectrum just prior to the addition of each new aliquot of base.[41]

Calculations of Equilibrium Constants: Equilibrium constants were generally calculated as concentration quotients (pH = –log[H^+]) using the computer programs HYPERQUAD and SPECFIT.[42,43] The total concentrations of the reactants and the pK_w (13.78 for μ = 0.1 M, 13.77 for μ = 1.0 M)[20] were not refined. The protonation constants of the diazepane ligand were evaluated separately and were kept fixed when refining formation constants of the metal-containing species. The UV/Vis spectra of the free Ni^{2+} and Cu^{2+} were recorded separately and were imported as fixed data sets for the evaluation of the formation constants of the metal complexes. The free ligand and its protonation products were treated as nonabsorbing species.

***N*^{1},*N*^{2}-Ditosyl-1,2-ethanediamine:**[44] Toluene-4-sulfonyl chloride (95 g, 0.5 mol) was suspended in diethyl ether (200 mL). The suspension was cooled with an ice bath, and a mixture of NaOH (20 g, 0.5 mol) and ethane-1,2-diamine (15 g, 0.25 mol, dissolved in 200 mL of H_2O) was added dropwise. The resulting white suspension was stirred overnight at room temperature. The residue was filtered off and recrystallized from MeOH (white crystals, 86.2 g, 94%). $C_{16}H_{20}N_2O_4S_2$ (368.5): calcd. C 52.15, H 5.47, N 7.60; found C 52.66, H 5.41, N 7.46. ^1H NMR (DMSO): δ = 2.39 (s, 6 H), 2.72 (s, 4 H), 7.38 (d, *J* = 8.2 Hz, 4 H), 7.61 (d, *J* = 8.2 Hz, 4 H) ppm. ^{13}C NMR (DMSO): δ = 21.0, 42.2, 126.5, 129.7, 137.4, 142.8 ppm. IR: $\tilde{\nu}$ = 664, 709, 748, 818, 875, 1020, 1058, 1092, 1153, 1188, 1240, 1292, 1307, 1330, 1404, 1452, 1496, 1598, 3282 cm^{-1}.

Disodium *N*^{1},*N*^{2}-Ditosyl-1,2-ethanediamide: Sodium metal (4.6 g, 0.2 mol) was allowed to react with water-free MeOH (150 mL), then *N*^{1},*N*^{2}-ditosyl-1,2-ethanediamine (36.8 g, 0.1 mol) was added. The white suspension was refluxed for half an hour, the solvent evaporated completely and the remaining white residue dried in vacuo (40.0 g, 97%). $C_{16}H_{18}N_2Na_2O_4S_2$ (412.4): calcd. C 46.60, H 4.40, N 6.79; found C 46.76, H 4.77, N 6.70. ^1H NMR (DMSO): δ = 2.32 (s, 6 H), 2.58 (s, 4 H), 7.18 (d, *J* = 8.0 Hz, 4 H), 7.50 (d, *J* = 8.0 Hz, 4 H) ppm. ^{13}C NMR (DMSO): δ = 20.9, 46.3, 126.4, 128.6, 139.2, 142.6 ppm. IR: $\tilde{\nu}$ = 658, 708, 811, 844, 884, 982, 1072, 1117, 1153 cm^{-1}.

1,4-Ditosyl-1,4-diazepan-6-ol:[18] Powdered KOH (1.9 g, 0.034 mol) was dissolved in absolute EtOH (250 mL) and 2,3-dibromo-1-propanol (3.5 mL, 0.034 mol) was added dropwise to this solution. The resulting white suspension was refluxed and disodium *N*^{1},*N*^{2}-ditosyl-1,2-ethanediamide (14 g, 0.034 mol) was added. The mixture was refluxed for an additional six hours and the remaining solid was removed from the boiling solution by filtration. The clear solution was then cooled to 4 °C, yielding 10.1 g (70%) of colorless crystals, which were filtered off and dried in vacuo. $C_{19}H_{24}N_2O_5S_2$ (424.5): calcd. C 53.75, H 5.70, N 6.60; found C 53.38, H 5.52, N 6.31. ^1H NMR (DMSO): δ = 2.39 (s, 6 H), 2.85 (dd, *J* = 13.9, 8.1 Hz, 2 H), 3.11 (m, 2 H), 3.48 (m, 4 H), 3.75 (sept, *J* = 4.2 Hz, 1 H), 5.28 (br., 1 H), 7.42 (d, *J* = 8.2 Hz, 4 H), 7.67 (d, *J* = 8.1 Hz, 4 H) ppm. ^{13}C NMR (DMSO): δ = 20.9, 49.0, 53.0, 68.4, 126.6, 129.8, 135.5, 143.3 ppm. IR: $\tilde{\nu}$ = 610, 653, 722, 805, 911, 972, 1036, 1086, 1151, 1266, 1330, 1400, 1442, 1493, 1598, 2922, 3502 cm^{-1}.

1,4-Ditosyl-1,4-diazepan-6-mesylate: 1,4-Ditosyl-1,4-diazepan-6-ol (10 g, 0.024 mol) was dissolved in anhydrous pyridine (50 mL) and cooled to 0 °C with an ice bath. Methanesulfonyl chloride (1.87 mL, 0.024 mol) was then added dropwise to this solution. A yellow solid precipitated, and the suspension was stirred for an additional 2 h at 0 °C. 3 M HCl (200 mL) was then added and the solid turned white. Stirring was continued for a further 2 h at 0 °C. The residue was then filtered off and washed with H_2O. The solid was extracted with boiling EtOH and dried in vacuo. Yield: 10.6 g (88%). $C_{20}H_{26}N_2O_7S_3$ (502.6): calcd. C 47.79, H 5.21, N 5.57; found C 47.77, H 5.19, N 5.63. ^1H NMR (DMSO): δ = 2.39 (s, 6 H), 3.23 (m, 2 H), 3.27 (s, 3 H), 3.37 (m, 2 H), 3.53 (d, *J* = 5.1 Hz, 4 H), 4.87 (quint, *J* = 5.1 Hz, 1 H), 7.42 (d, *J* = 8.2 Hz, 4 H), 7.69 (d, *J* = 8.2 Hz, 4 H) ppm. ^{13}C NMR: δ = 20.9, 37.8, 50.4, 51.2, 76.7, 126.7, 129.9, 135.3, 143.6 ppm. IR: $\tilde{\nu}$ = 570, 619, 652, 702,

715, 743, 807, 904, 916, 949, 974, 1001, 1074, 1090, 1148, 1161, 1282, 1310, 1331, 1347, 1442, 1496, 1598 cm^{-1}.

6-Azido-1,4-ditosyl-1,4-diazepane: *Caution: Organic azides are potentially explosive. These must be handled with care and should not be isolated in large amounts*![19] Solid 1,4-ditosyl-1,4-diazepan-6-mesylate (5 g, 0.01 mol) was added to a solution of NaN_3 (1.95 g, 0.03 mol) in absolute DMF (100 mL). The resulting white suspension was heated to 100–110 °C for 48 h. A white solid was removed by filtration, yielding a clear, yellow solution of the desired product. A small sample to be used for IR and NMR characterization was precipitated by the addition of H_2O to a few milliliters of the DMF solution. The resulting white solid was separated by filtration and air-dried. ^1H NMR (DMSO): δ = 2.40 (s, 6 H), 3.19 (m, 2 H), 3.39 (m, 6 H), 3.89 (m, 1 H), 7.43 (d, J = 8.3 Hz, 4 H), 7.69 (d, J = 8.3 Hz, 4 H) ppm. ^{13}C NMR (DMSO): δ = 20.9, 50.1, 50.9, 58.6, 127.0, 130.1, 135.5, 143.7 ppm. IR: $\tilde{\nu}$ = 656, 696, 720, 813, 860, 909, 958, 1036, 1090, 1158, 1245, 1306, 1332, 1381, 1455, 1494, 1599, 2110 cm^{-1}. The crystal structure has been published in a previous communication.[45]

1,4-Ditosyl-1,4-diazepan-6-amine: The experiment reported in the previous section was repeated one more time and the resulting DMF solutions of the azide were combined to one single solution. This solution was then transferred into an autoclave and hydrogenated (5 atm H_2) using 10% Pd/C (500 mg) as catalyst. After 48 h the catalyst was removed by filtration and the resulting solution (300 mL) was diluted with 1 L of H_2O. The white solid that precipitated was filtered off and dried in vacuo. This product proved to be of sufficient purity to be used for the next step, however the elemental analysis was not satisfactory. The product could be isolated as analytically pure hydrobromide by dissolving the amine in EtOH (100 mL) and adding aqueous concd. HBr (10 mL). The resulting yellow solution was filtered through Celite and the solvents evaporated to dryness. A colorless solid was obtained which was dried in vacuo (7.1 g, 70%). $C_{19}H_{25}N_3S_2O_4{\cdot}HBr$ (504.5): calcd. C 45.24, H 5.19, N 8.33; found C 45.34, H 5.38, N 8.06. ^1H NMR (DMSO): δ = 3.40 (m, 3 H), 3.45 (m, 4 H), 3.63 (dd, J = 14.4, J = 4.1 Hz, 2 H), 7.47 (d, J = 8.2 Hz, 4 H), 7.72 (d, J = 8.2 Hz, 4 H) ppm. ^{13}C NMR (DMSO): δ = 20.9, 48.9, 49.4, 50.0, 126.6, 130.1, 134.9, 143.8 ppm. IR: $\tilde{\nu}$ = 571, 653, 721, 813, 905, 967, 1030, 1089, 1152, 1330, 1449, 1494, 1597 cm^{-1}. The crystal structure of the free amine has been published in a previous communication.[46]

1,4-Diazepan-6-amine·3HBr: 1,4-Ditosyl-1,4-diazepan-6-amine (5 g, 0.012 mol) was refluxed in concd. aqueous HBr (150 mL) for 3 h. The solution was cooled to room temperature and was then concentrated to a volume of 50 mL on a rotary evaporator. A white solid crystallized which was filtered off and washed with cold EtOH. Drying in vacuo yielded 3.2 g of the trihydrobromide salt (75%). $C_5H_{16}Br_3N_3$ (357.9): calcd. C 16.78, H 4.51, N 11.74; found C 16.87, H 4.58 N 11.74. ^1H NMR (D_2O, pH < 3): δ = 3.67 (dd, J = 14.1, J = 10.5 Hz, 2 H), 3.77 (m, 4 H), 3.89 (dd, J = 14.1, J = 3.1 Hz, 2 H), 4.26 (tt, J = 10.5, J = 3.1 Hz, 1 H) ppm. ^{13}C NMR (D_2O, pH < 3): δ = 45.9, 47.1, 49.3 ppm. IR: $\tilde{\nu}$ = 767, 844, 864, 882, 910, 991, 1020, 1050, 1127, 1180, 1265, 1298, 1326, 1392, 1429, 1447, 1465, 1524, 1548, 2781 cm^{-1}.

1,4-Diazepan-6-amine·3HCl·1.5H$_2$O: This compound was obtained from the trihydrobromide by ion-exchange chromatography on Dowex 50. $C_5H_{16}N_3Cl_3{\cdot}1.5H_2O$ (251.6): calcd. C 23.87, H 7.61, N 16.70; found C 23.45, H 7,88, N 17.09. The ^1H and ^{13}C NMR spectra were identical with those of the trihydrobromide. IR: $\tilde{\nu}$ = 773, 852, 868, 890, 1000, 1055, 1092, 1135, 1199, 1234, 1271, 1396, 1435, 1539, 2718 cm^{-1}. Single crystals of composition $H_3dazaCl_3{\cdot}H_2O$, suitable for X-ray analysis were grown by slow evaporation of an aqueous solution.

[Co(daza)$_2$]Cl$_3$: 1,4-Diazepan-6-amine·3HBr (2.5 g, 7.0 mmol) was dissolved in H_2O (50 mL), and the pH of the solution was adjusted to 8.5 by adding NaOH (1 M). Solid $CoCl_2{\cdot}6H_2O$ (0.83 g, 3.5 mmol) was then added, resulting in a red-orange solution, which was stirred in an open beaker for 3 d. The solution was tested for Co^{2+} (negative), and sorbed onto Dowex 50. The column was washed successively with H_2O (500 mL), aqueous 0.5 M HCl (500 mL), and aqueous 1 M HCl (500 mL). The product was then eluted from the column with aqueous 3 M HCl (500 mL). The last fraction was evaporated to dryness, and the resulting orange solid was dissolved in a small amount of H_2O and sorbed onto a column of SP-Sephadex C-25 (column length: 2 m). The column was eluted with trisodium citrate (0.2 M). Beside several minor bands, two major orange bands ($\mathbf{1}^{3+}$, $\mathbf{2}^{3+}$) were observed. The two major bands were collected separately, desalted on Dowex 50 (3 M HCl), and the solvents evaporated to dryness.

***trans*-[Co(daza)$_2$]Cl$_3$·4H$_2$O (1Cl$_3$·4H$_2$O):** Yield: 25%. $C_{10}H_{26}CoCl_3N_6{\cdot}4H_2O$ (467.7): calcd. C 25.68, H 7.33, N 17.97; found C 25.75, H 7.11, N 18.52. ^1H NMR (D_2O): δ = 2.69 (d, J = 13.4 Hz, 4 H), 2.88 (d, J = 8.3 Hz, 4 H), 3.42 (br. s, 2 H), 3.43 (m, 4 H), 3.62 (d, J = 13.4 Hz, 4 H) ppm. ^{13}C NMR (D_2O): δ = 55.7, 56.9, 62.3 ppm. IR: $\tilde{\nu}$ = 626, 780, 884, 981, 1044, 1092, 1128, 1183, 1231, 1314, 1379, 1417, 1614, 2114, 3032 cm^{-1}. UV/Vis: λ_{max} (ε) = 335 nm (75), 470 (79).

***cis*-[Co(daza)$_2$]Cl$_3$·1.5H$_2$O (2Cl$_3$·1.5H$_2$O):** Yield: 20%. $C_{10}H_{26}Cl_3CoN_6{\cdot}1.5H_2O$ (422.7): calcd. C 28.42, H 6.92, N 19.88; found C 28.21, H 6.85, N 19.91. ^1H NMR (D_2O): δ = 2.71 (d, J = 13.5 Hz, 4 H), 3.04 (m, 4 H), 3.44 (m, 4 H), 3.49 (br. s, 2 H), 3.56 (d, J = 13.5 Hz, 2 H), 3.78 (m, 2 H) ppm. ^{13}C NMR (D_2O): δ = 55.6, 56.3, 57.4, 61.9 (two C atoms) ppm. IR: $\tilde{\nu}$ = 886, 988, 1048, 1092, 1151, 1230, 1285, 1316, 1356, 1444, 1496, 1590, 1981, 2051, 2165, 2323, 2430, 2754, 2875, 3030 cm^{-1}. UV/Vis: λ_{max} (ε) = 345 nm (140), 470 (157).

Single crystals: $\mathbf{1}Cl_3{\cdot}4H_2O$ (24 mg) and $\mathbf{2}Cl_3{\cdot}1.5H_2O$ (24 mg) were separately dissolved in H_2O. $ZnBr_2$ (59 mg, 0.26 mmol) was added to each of the solutions. The solutions were acidified with 3 M aqueous HBr to pH < 1. Slow evaporation yielded orange crystals of composition $[\mathbf{1}]_3(ZnBr_4)_2Br_5{\cdot}4\,H_2O$ and $[\mathbf{2}](ZnBr_4)Br{\cdot}H_2O$, suitable for X-ray analysis.

[Cu(daza)Cl$_2$]: 1,4-Diazepan-6-amine·3HCl·H$_2$O (100 mg, 0.41 mmol) was dissolved in 1 mL of H_2O. $CuCl_2{\cdot}2H_2O$ (35 mg, 0.21 mmol) was added to this solution, and the pH was adjusted to 7 with 0.5 M NaOH (2 mL). The solution was then diluted with EtOH and was allowed to stand at 4 °C for a few days, yielding a small number of blue crystals which were suitable for the single crystal analysis. IR: $\tilde{\nu}$ = 666, 768, 853, 872, 966, 1041, 1098, 1149, 1319, 1444, 1605, 2848, 2871, 3167, 3242, 3300, 3322 cm^{-1}.

[Ni(daza)$_2$]Cl$_2$·3.2H$_2$O: 1,4-Diazepan-6-amine·3HCl·H$_2$O (100 mg, 0.41 mmol) was dissolved in 1 mL of H_2O. Solid $NiCl_2{\cdot}6H_2O$ (50 mg, 0.21 mmol) was then added and the pH was adjusted to 8 with 0.1 M KOH (12 mL). The resulting purple solution was allowed to evaporate slowly over a period of several days at room temperature, yielding a small number of purple crystals suitable for the X-ray analysis. IR: $\tilde{\nu}$ = 628, 914, 965, 1043, 1064, 1099, 1143, 1614 br, 2875, 3166, 3227, 3313 cm^{-1}.

[Zn(daza)$_2$]SO$_4$·5H$_2$O: 1,4-Diazepan-6-amine·3HBr (200 mg, 0.56 mmol) was deprotonated on Dowex 2 (OH^- form). The volume of the resulting solution was reduced to 10 mL. Solid $ZnSO_4{\cdot}7H_2O$ (81 mg, 0.28 mmol) was added, and the solution was

Table 7. Crystallographic data for daza·3HCl·H_2O, [$CuLCl_2$], [$Ni(L)_2$]Cl_2·3.2H_2O, [$Zn(L)_2$]SO_4·5H_2O, *trans*-[$Co(L)_2$]$_3$($ZnBr_4$)$_2Br_5$·4H_2O, and *cis*-[$Co(L)_2$]($ZnBr_4$)Br·H_2O.

	daza·3HCl·H_2O	[$Ni(L)_2$]Cl_2·3.2H_2O	[$CuLCl_2$]	[$Zn(L)_2$]SO_4·5H_2O	**1**$_3$($ZnBr_4$)$_2Br_5$·4H_2O	**2**($ZnBr_4$)Br·H_2O
Formula	$C_5H_{18}Cl_3N_3O$	$C_{10}H_{32.4}Cl_2N_6NiO_{3.2}$	$C_5H_{13}Cl_2N_3Cu$	$C_{10}H_{36}N_6O_9SZn$	$C_{30}H_{86}Br_{13}Co_3N_{18}O_4Zn_2$	$C_{10}H_{28}Br_5CoN_6OZn$
M_w	242.57	417.63	249.62	481.88	2109.54	772.23
T [K]	200(2)	293(2)	200(2)	293(2)	100(2)	100(2)
Crystal system	monoclinic	monoclinic	orthorhombic	triclinic	orthorhombic	orthorhombic
Space group	$P2_1/n$	$P2_1/n$	$Pna2_1$	$P\bar{1}$	$Pbcn$	$Pnma$
a [Å]	12.500(2)	8.708(2)	16.715(3)	8.366(2)	15.8270(4)	26.8941(12)
b [Å]	6.8580(10)	8.826(2)	6.9430(10)	9.065(2)	23.5711(6)	8.4372(4)
c [Å]	14.061(3)	12.480(2)	7.918(2)	15.450(3)	16.0633(5)	9.5817(4)
α [°]	90.00	90.00	90.00	91.09(3)	90.00	90.00
β [°]	112.56(3)	97.59(3)	90.00	101.97(3)	90.00	90.00
γ [°]	90.00	90.00	90.00	115.54(3)	90.00	90.00
V [Å^3]	1113.1(3)	950.8(3)	918.9(3)	1026.4(4)	5992.6(3)	2174.19(17)
Z	4	2	4	2	4	4
$\rho_{calcd.}$ [g cm^{-3}]	1.447	1.459	1.804	1.559	2.338	2.359
μ [mm^{-1}]	0.788	1.322	2.899	1.352	10.322	11.067
min./max. transm.	–	–	–	0.5931/0.9977	0.0769/0.4783	0.2882/0.5960
Crystal size [mm]	0.3×0.3×0.2	0.4×0.3×0.2	0.20×0.15×0.15	0.30×0.25×0.15	0.34×0.26×0.07	0.16×0.10×0.05
θ range [°]	1.86–24.06	2.69–25.00	2.44–24.06	2.51–25.00	3.68–29.00	2.61–28.04
hkl ranges	–14/13	–10/10	–18/18	–9/9	–21/21	–35/35
	–7/7	0/10	–7/7	–10/10	–32/32	–11/11
	–15/15	0/14	–9/9	0/18	–20/14	–12/12
Measured refl.	6690	1674	5321	3603	30240	21318
Unique refl.	1682	1674	1385	3603	7545	2796
Obsd. refl.[a]	1177	1533	879	3381	6405	2550
Parameters	181	162	100	383	343	188
R_1,wR_2 [$I > 2\sigma(I)$]	0.0295, 0.0575	0.0550, 0.1277	0.0539, 0.1166	0.0402, 0.1031	0.0364, 0.0799	0.0491, 0.0946
R_1,wR_2 (all data)	0.0535, 0.0629	0.0579, 0.1334	0.0904, 0.1265	0.0427, 0.1062	0.0467, 0.0850	0.0556, 0.0967

[a] For $I > 2\sigma(I)$.

layered with acetone, yielding single crystals suitable for X-ray analysis.

Single Crystal X-ray Diffraction Studies:[47] Data sets were collected on the following diffractometers: STOE IPDS (daza·3HCl·H_2O and [$Cu(daza)Cl_2$]), STOE STADI-4 ([$Ni(daza)_2$]Cl_2·3.2H_2O and [$Zn(daza)_2$]SO_4·5H_2O), Nonius Kappa-CCD (*trans*-[$Co(daza)_2$]$_3$-($ZnBr_4$)$_2Br_5$·4H_2O, and *cis*-[$Co(daza)_2$]($ZnBr_4$)Br·H_2O). Graphite-monochromated Mo-K_α radiation (λ = 0.71073 Å) was used throughout. The data for the two Co complexes were collected at 100(2) K, daza·3HCl·H_2O and [$Cu(daza)Cl_2$] were measured at 200(2) K, and the other data sets were collected at ambient temperature. An absorption correction was performed for *cis*-[Co-($daza)_2$]($ZnBr_4$)Br·H_2O (face-indexed numerical), *trans*-[Co-($daza)_2$]$_3$($ZnBr_4$)$_2Br_5$·4H_2O (faced-indexed numerical), and [$Zn(daza)_2$]SO_4·5H_2O (empirical). Further details of data collection and structure solution are summarized in Table 7. The structures were solved by direct methods (SHELXS-97) and refined by full-matrix, least-squares calculations on F^2 using SHELXL-97.[48] Anisotropic displacement parameters were refined for all non-hydrogen atoms. The hydrogen atoms of daza·3HCl·H_2O, [$Zn(daza)_2$]-SO_4·5H_2O, and [$Ni(daza)_2$]Cl_2·3.2H_2O were located and refined isotropically. The H-atom positions of the other complexes were calculated (riding model). The disorder problems of the Co complexes **1**a^{3+} and **2**$^{3+}$ are described in detail in Section 2.2. In the structure of **2**$^{3+}$, a total of 21 restraints was used to adjust corresponding bond lengths and angles of the two ligands to the same value within suitable limits (SAME instruction of SHELXL-97). Puckering parameters were calculated using the computer program PLATON.[49]

Acknowledgments

X-ray diffraction data of $H_3dazaCl_3$·H_2O and of the Ni, Cu, and Zn complexes were recorded by Dr. Volker Huch (Saarbrücken). We thank Dr. Peter Osvath (Melbourne) for valuable advice. Financial support by the Deutsche Forschungsgemeinschaft is gratefully acknowledged.

[1] a) R. F. Childers, R. A. D. Wentworth, L. J. Zompa, *Inorg. Chem.* **1971**, *10*, 302, and references cited therein; b) W. A. Freeman, C. F. Liu, *Inorg. Chem.* **1975**, *14*, 2120; c) D. Parker, K. Senanayake, J. Vepsailainen, S. Williams, A. S. Batsanov, J. A. K. Howard, *J. Chem. Soc., Perkin Trans. 2* **1997**, 1445; d) F. M. Menger, J. Bian, V. A. Azov, *Angew. Chem. Int. Ed.* **2002**, *41*, 2581; e) L. Turculet, T. D. Tilley, *Organometallics* **2004**, *23*, 1542.

[2] K. Hegetschweiler, *Chem. Soc. Rev.* **1999**, *28*, 239.

[3] M. Ghisletta, L. Hausherr-Primo, K. Gajda-Schrantz, G. Machula, L. Nagy, H. W. Schmalle, G. Rihs, F. Endres, K. Hegetschweiler, *Inorg. Chem.* **1998**, *37*, 997.

[4] a) J. Sander, K. Hegetschweiler, B. Morgenstern, A. Keller, W. Amrein, T. Weyhermüller, I. Müller, *Angew. Chem. Int. Ed.* **2001**, *40*, 4180; b) K. Hegetschweiler, R. C. Finn, R. S. Rarig Jr., J. Sander, S. Steinhauser, M. Wörle, J. Zubieta, *Inorg. Chim. Acta* **2002**, *337*, 39; c) D. Chapon, J.-P. Morel, P. Delangle, C. Gateau, J. Pécaut, *Dalton Trans.* **2003**, 2745; d) B. Morgenstern, S. Steinhauser, K. Hegetschweiler, E. Garribba, G. Micera, D. Sanna, L. Nagy, *Inorg. Chem.* **2004**, *43*, 3116; e) K. Hegetschweiler, B. Morgenstern, J. Zubieta, P. J. Hagrman, N. Lima, R. Sessoli, F. Totti, *Angew. Chem. Int. Ed.* **2004**, *43*, 3436; f) K. Hegetschweiler, A. Egli, E. Herdtweck, W. A.

Herrmann, R. Alberto, V. Gramlich, *Helv. Chim. Acta* **2005**, *88*, 426.
[5] P. Chaudhuri, K. Wieghardt, *Prog. Inorg. Chem.* **1987**, *35*, 329.
[6] a) J. H. Koek, S. W. Russell, L. van der Wolf, R. Hage, J. B. Warnaar, A. L. Spek, J. Kerschner, L. Del Pizzo, *J. Chem. Soc., Dalton Trans.* **1996**, 353; b) A. C. Moreland, T. B. Rauchfuss, *J. Am. Chem. Soc.* **1998**, *120*, 9376; c) C. Bolm, N. Meyer, G. Raabe, T. Weyhermüller, E. Bothe, *Chem. Commun.* **2000**, 2435; d) L. D. Slep, A. Mijovilovich, W. Meyer-Klaucke, T. Weyhermüller, E. Bill, E. Bothe, F. Neese, K. Wieghardt, *J. Am. Chem. Soc.* **2003**, *125*, 15554.
[7] a) G. Park, J. Shao, F. H. Lu, R. D. Rogers, N. D. Chasteen, M. W. Brechbiel, R. P. Planalp, *Inorg. Chem.* **2001**, *40*, 4167; b) E. A. Lewis, H. H. Khodr, R. C. Hider, J. R. Lindsay Smith, P. H. Walton, *Dalton Trans.* **2004**, 187; c) E. Boseggia, M. Gatos, L. Lucatello, F. Mancin, S. Moro, M. Palumbo, C. Sissi, P. Tecilla, U. Tonellato, G. Zagotto, *J. Am. Chem. Soc.* **2004**, *126*, 4543; d) C. Sissi, F. Mancin, M. Gatos, M. Palumbo, P. Tecilla, U. Tonellato, *Inorg. Chem.* **2005**, *44*, 2310.
[8] a) U. Bossek, T. Weyhermüller, K. Wieghardt, B. Nuber, J. Weiss, *J. Am. Chem. Soc.* **1990**, *112*, 6387; b) U. Bossek, M. Saher, T. Weyhermüller, K. Wieghardt, *J. Chem. Soc., Chem. Commun.* **1992**, 1780; c) U. Bossek, H. Hummel, T. Weyhermüller, E. Bill, K. Wieghardt, *Angew. Chem. Int. Ed. Engl.* **1995**, *34*, 2642.
[9] a) R. A. D. Wentworth, P. S. Dahl, C. J. Huffman, W. O. Gillum, W. E. Streib, J. C. Huffman, *Inorg. Chem.* **1982**, *21*, 3060; b) J. E. Bollinger, J. T. Mague, W. A. Banks, A. J. Kastin, D. M. Roundhill, *Inorg. Chem.* **1995**, *34*, 2143; c) P. Caravan, C. Orvig, *Inorg. Chem.* **1997**, *36*, 236; d) H. Luo, N. Eberly, R. D. Rogers, M. W. Brechbiel, *Inorg. Chem.* **2001**, *40*, 493; e) A. K. Nairn, R. Bhalla, S. P. Foxon, X. Liu, L. J. Yellowlees, B. C. Gilbert, P. H. Walton, *J. Chem. Soc., Dalton Trans.* **2002**, 1253; f) N. Ye, G. Park, A. M. Przyborowska, P. E. Sloan, T. Clifford, C. B. Bauer, G. A. Broker, R. D. Rogers, R. Ma, S. V. Torti, M. W. Brechbiel, R. P. Planalp, *Dalton Trans.* **2004**, 1304.
[10] a) K. Hegetschweiler, A. Egli, R. Alberto, H. W. Schmalle, *Inorg. Chem.* **1992**, *31*, 4027; b) A. Kramer, R. Alberto, A. Egli, I. Novak-Hofer, K. Hegetschweiler, U. Abram, P. V. Bernhardt, P. A. Schubiger, *Bioconjugate Chem.* **1998**, *9*, 691.
[11] a) A. E. Martell, R. J. Motekaitis, M. J. Welch, *J. Chem. Soc., Chem. Commun.* **1990**, 1748; b) C. Stockheim, L. Hoster, T. Weyhermüller, K. Wieghardt, B. Nuber, *J. Chem. Soc., Dalton Trans.* **1996**, 4409; c) R. Schnepf, A. Sokolowski, J. Müller, V. Bachler, K. Wieghardt, P. Hildebrandt, *J. Am. Chem. Soc.* **1998**, *120*, 2352; d) S. J. Brudenell, L. Spiccia, A. M. Bond, G. D. Fallon, D. C. R. Hockless, G. Lazarev, P. J. Mahon, E. R. T. Tiekink, *Inorg. Chem.* **2000**, *39*, 881; e) P. C. McGowan, T. J. Podesta, M. Thornton-Pett, *Inorg. Chem.* **2001**, *40*, 1445; f) V. Pavlishchuk, F. Birkelbach, T. Weyhermüller, K. Wieghardt, P. Chaudhuri, *Inorg. Chem.* **2002**, *41*, 4405; g) M. Li, D. Bonnet, E. Bill, F. Neese, T. Weyhermüller, N. Blum, D. Sellmann, K. Wieghardt, *Inorg. Chem.* **2002**, *41*, 3444; h) A. L. Gott, P. C. McGowan, T. J. Podesta, C. W. Tate, *Inorg. Chim. Acta* **2004**, *357*, 689.
[12] a) H. Manohar, D. Schwarzenbach, *Helv. Chim. Acta* **1974**, *57*, 519; b) H. Manohar, D. Schwarzenbach, W. Iff, G. Schwarzenbach, *J. Coord. Chem.* **1979**, *8*, 213.
[13] a) G. Seeber, A. L. Pickering, D.-L. Long, L. Cronin, *Chem. Commun.* **2003**, 2002; b) A. L. Pickering, D.-L. Long, L. Cronin, *Inorg. Chem.* **2004**, *43*, 4953.
[14] J. W. Pauly, J. Sander, D. Kuppert, M. Winter, G. J. Reiss, F. Zürcher, R. Hoffmann, T. F. Fässler, K. Hegetschweiler, *Chem. Eur. J.* **2000**, *6*, 2830.
[15] D. Kuppert, J. Sander, C. Roth, M. Wörle, T. Weyhermüller, G. J. Reiss, U. Schilde, I. Müller, K. Hegetschweiler, *Eur. J. Inorg. Chem.* **2001**, 2525.
[16] S. Aime, L. Calabi, C. Cavallotti, E. Gianolio, G. B. Giovenzana, P. Losi, A. Maiocchi, G. Palmisano, M. Sisti, *Inorg. Chem.* **2004**, *43*, 7588.
[17] a) S. Kato, H. Harada, T. Morie, *J. Chem. Soc., Perkin Trans. 1* **1997**, 3219; b) Y. Hirokawa, I. Fujiwara, K. Suzuki, H. Harada, T. Yoshikawa, N. Yoshida, S. Kato, *J. Med. Chem.* **2003**, *46*, 702.
[18] W. S. Saari, A. W. Raab, S. W. King, *J. Org. Chem.* **1971**, *36*, 1711.
[19] E. B. Fleischer, A. E. Gebala, A. Levey, P. A. Tasker, *J. Org. Chem.* **1971**, *36*, 3042.
[20] R. M. Smith, A. E. Martell, R. J. Motekaitis, *Critically Selected Stability Constants of Metal Complexes*, NIST Standard Reference Database 46; Version 8.0; Gaithersburg, MD, USA **2004**.
[21] M. Weber, D. Kuppert, K. Hegetschweiler, V. Gramlich, *Inorg. Chem.* **1999**, *38*, 859.
[22] R. Yang, L. J. Zompa, *Inorg. Chem.* **1976**, *15*, 1499.
[23] K. Hegetschweiler, O. Maas, A. Zimmer, R. J. Geue, A. M. Sargeson, J. Harmer, A. Schweiger, I. Buder, G. Schwitzgebel, V. Reiland, W. Frank, *Eur. J. Inorg. Chem.* **2003**, 1340.
[24] In this paper, the term pH* refers to the direct pH Meter reading for D_2O samples (no inert electrolyte) using a pH electrode with an aqueous (H_2O) reference which was calibrated with aqueous (H_2O) buffer solutions. For the interconversion of pH* and pD see: a) R. Delgado, J. J. R. Frausto Da Silva, M. T. S. Amorim, M. F. Cabral, S. Chaves, J. Costa, *Anal. Chim. Acta* **1991**, *245*, 271; b) Z. Szakacs, G. Hägele, R. Tyka, *Anal. Chim. Acta* **2004**, *522*, 247.
[25] J. L. Sudmeier, C. N. Reilley, *Anal. Chem.* **1964**, *36*, 1698.
[26] M. Karplus, *J. Am. Chem. Soc.* **1963**, *85*, 2870.
[27] I. K. Boessenkool, J. C. A. Boeyens, *J. Cryst. Mol. Struct.* **1980**, *10*, 11.
[28] $\tau = (\alpha - \beta)/60$, where α is the largest and β is the second largest bond angle within the coordination sphere. $\tau = 1$ corresponds to trigonal bipyramidal and $\tau = 0$ to a square-pyramidal coordination, see: A. W. Addison, T. N. Rao, J. Reedijk, J. van Rijn, G. C. Verschoor, *J. Chem. Soc., Dalton Trans.* **1984**, 1349.
[29] a) R. F. Childers, R. A. D. Wentworth, *Inorg. Chem.* **1969**, *8*, 2218; b) G. Schwarzenbach, H.-B. Bürgi, W. P. Jensen, G. A. Lawrance, L. Mønsted, A. M. Sargeson, *Inorg. Chem.* **1983**, *22*, 4029.
[30] K. Hegetschweiler, V. Gramlich, M. Ghisletta, H. Samaras, *Inorg. Chem.* **1992**, *31*, 2341.
[31] A. Zimmer, D. Kuppert, T. Weyhermüller, I. Müller, K. Hegetschweiler, *Chem. Eur. J.* **2001**, *7*, 917.
[32] E. Prenesti, P. G. Daniele, M. Prencipe, G. Ostacoli, *Polyhedron* **1999**, *18*, 3233.
[33] J. Bjerrum, B. V. Agarwala, *Acta Chem. Scand.* **1980**, *A34*, 475.
[34] L. Fabbrizzi, M. Micheloni, P. Paoletti, *J. Chem. Soc., Dalton Trans.* **1980**, 1055.
[35] R. Pizer, *Inorg. Chem.* **1984**, *23*, 3027.
[36] K. Hegetschweiler, R. D. Hancock, M. Ghisletta, T. Kradolfer, V. Gramlich, H. W. Schmalle, *Inorg. Chem.* **1993**, *32*, 5273.
[37] a) C. K. Jørgensen, *Inorg. Chem.* **1964**, *3*, 1201; b) R. G. Pearson, *Inorg. Chem.* **1973**, *12*, 712.
[38] R. D. Hancock, *Acc. Chem. Res.* **1990**, *23*, 253.
[39] U. Brand, H. Vahrenkamp, *Inorg. Chim. Acta* **1992**, *198–200*, 663.
[40] C. Neis, Diploma Thesis, Saarbrücken, **2005**.
[41] S. Steinhauser, U. Heinz, M. Bartholomä, T. Weyhermüller, H. Nick, K. Hegetschweiler, *Eur. J. Inorg. Chem.* **2004**, 4177.
[42] P. Gans, A. Sabatini, A. Vacca, *Talanta* **1996**, *43*, 1739.
[43] a) R. A. Binstead, B. Jung, A. D. Zuberbühler, SPECFIT/32 Version 3.0, Spectrum Software Associates, Marlborough, MA **01752**, USA, **2000**; b) H. Gampp, M. Maeder, C. J. Meyer, A. D. Zuberbühler, *Talanta* **1985**, *32*, 95.
[44] H. Stetter, E.-E. Roos, *Chem. Ber.* **1954**, *87*, 566.
[45] J. Romba, S. Steinhauser, K. Hegetschweiler, *Z. Kristallogr. - New Cryst. Struct.* **2002**, *217*, 135.
[46] J. Romba, S. Steinhauser, K. Hegetschweiler, *Z. Kristallogr. - New Cryst. Struct.* **2002**, *217*, 133.

[47] CCDC-279823 to -279828 (for *cis*-[Co(daza)$_2$](ZnBr$_4$)Br·H$_2$O, *trans*-[Co(daza)$_2$]$_3$(ZnBr$_4$)$_2$Br$_5$·4H$_2$O, [Cu(daza)Cl$_2$], daza·3HCl·H$_2$O, [Zn(daza)$_2$]SO$_4$·5H$_2$O, and [Ni(daza)$_2$]Cl$_2$·3.2H$_2$O, respectively) contain the supplementary crystallographic data for this paper. These data can be obtained free of charge from The Cambridge Crystallographic Data Centre via www.ccdc.cam.ac.uk/data_request/cif.
[48] a) G. M. Sheldrick, SHELXS-97, *Program for Crystal Structure Solution*, Göttingen, **1990**; b) G. M. Sheldrick, SHELXL-97, *Program for Crystal Structure Refinement*, Göttingen, **1997**.
[49] A. L. Spek, PLATON, A Multipurpose Crystallographic Tool, Utrecht University, Utrecht, The Netherlands, **2005**; see also: A. L. Spek, *J. Appl. Cryst.* **2003**, *36*, 7.

Received: August 1, 2005
Published Online: December 1, 2005

